J. Nannoplankton Res., **42**(1), 2024, pp. 37–53 https://doi.org/10.58998/jnr3888
 ISSN 1210-8049 Printed by The Sheridan Press, USA

Oligocene–Early Miocene calcareous nannofossil biostratigraphy and paleoenvironment from the northern South China Sea

Changji Xuan
Shenzhen Branch of CNOOC Ltd./ CNOOC Deepwater Development Ltd., Shenzhen 518000, Guangdong, China

Yasu Wang
College of Oceanography, Hohai University, Nanjing 210024, China

Shijun Jiang*
College of Oceanography, Hohai University, Nanjing 210024, China; ssj0047@my.fsu.edu
Southern Marine Science and Engineering Guangdong Laboratory (Zhuhai), Zhuhai 519082, China

*Corresponding author

Manuscript received 16 January 2024; revised manuscript accepted 10 April 2024
Available online 10 June 2024
DOI: 10.58998/jnr3888

Abstract Calcareous nannofossil biostratigraphy is a powerful tool to date rock cuttings typically collected during drilling operations by the oil industry. However, there is limited information available for the international community on the application of nannofossil biostratigraphy in the northern South China Sea (SCS) owing to the scarcity of related publications. Here we present a case study of calcareous nannofossil biostratigraphy and paleoenvironmental interpretation of a deep-water exploration well (L1) located on the northern shelf of the SCS. Our analysis identified a series of last occurrence (LO) datums of zonal markers including *Sphenolithus belemnos*, *Triquetrorhabdulus carinatus*, *Reticulofenestra bisecta* (>10 μm), and *Sphenolithus* (=*Furcatolithus*) *distentus*, establishing nannofossil Zones NP24–NN4, as well as a number of supplementary secondary LO datums (e.g., *Sphenolithus delphix*, *Sphenolithus* [=*Furcatolithus*] *predistentus*). This biostratigraphy dates the studied section between 4650 and 2730 m below the seafloor to the Oligocene to Early Miocene. Interval III (4650–3980 m), which is late Oligocene or older in age, corresponds to a shallow water depositional environment, with large amounts of terrestrial clastic material, high sedimentation rates, and a near absence of nannofossils due to dilution. Interval II (3970–3012 m) is characterized by an unstable environment due to notably fluctuating sea levels, and also contains a widespread erosion horizon in the SCS across the Oligocene/Miocene boundary. Lower Miocene Interval I (3000–2730 m) has the highest values of total abundance, diversity, and number of *Discoaster* specimens, suggesting a stable, open-ocean environment and corresponding to a relatively low sedimentation rate.

Keywords Calcareous nannofossil, Early Miocene, Oligocene, Pearl River Mouth Basin, northern South China Sea

1. Introduction

Calcareous nannofossils are tiny microfossils generally smaller than 30 μm in size composed of calcite, which are produced by a diverse group of marine haptophyte algae (Haq, 1983; Winter & Siesser, 1994; Bown, 1998). This heterogeneous group of marine phytoplankton originated in the Late Triassic, radiated in the Jurassic, and dominated the planktonic marine biosphere from the Jurassic through Paleogene (Bown, 2005; De Vargas et al., 2007). Their modern representatives, coccolithophores, are characteristically single-celled, autotrophic, calcifying organisms that typically encase their cell walls with calcite ($CaCO_3$) plates called coccoliths. Marine phytoplankton play a crucial role in the biological pump for the global carbon cycle through carbon fixation and carbonate production (Winter & Siesser, 1994; Billard & Inouye, 2004; Rost & Riebesell, 2004; Young et al., 2005; Taylor et al., 2017). Due to their small size, high abundance, rapid evolution, and global distribution through geological time, calcareous nannofossils arguably have the most complete fossil record and have been extensively utilized in biostratigraphy and paleoceanography (Mutterlose et al., 2005; Agnini et al., 2017). Specifically, marine strata have been subdivided into zones/subzones based on nannofossil evolutionary originations and demise of certain species for both the Mesozoic (see Bown, 1998 for a review) and Cenozoic, including the zonation scheme of Martini (1971), which was further refined by Backman et al. (2012) and Agnini et al. (2014).

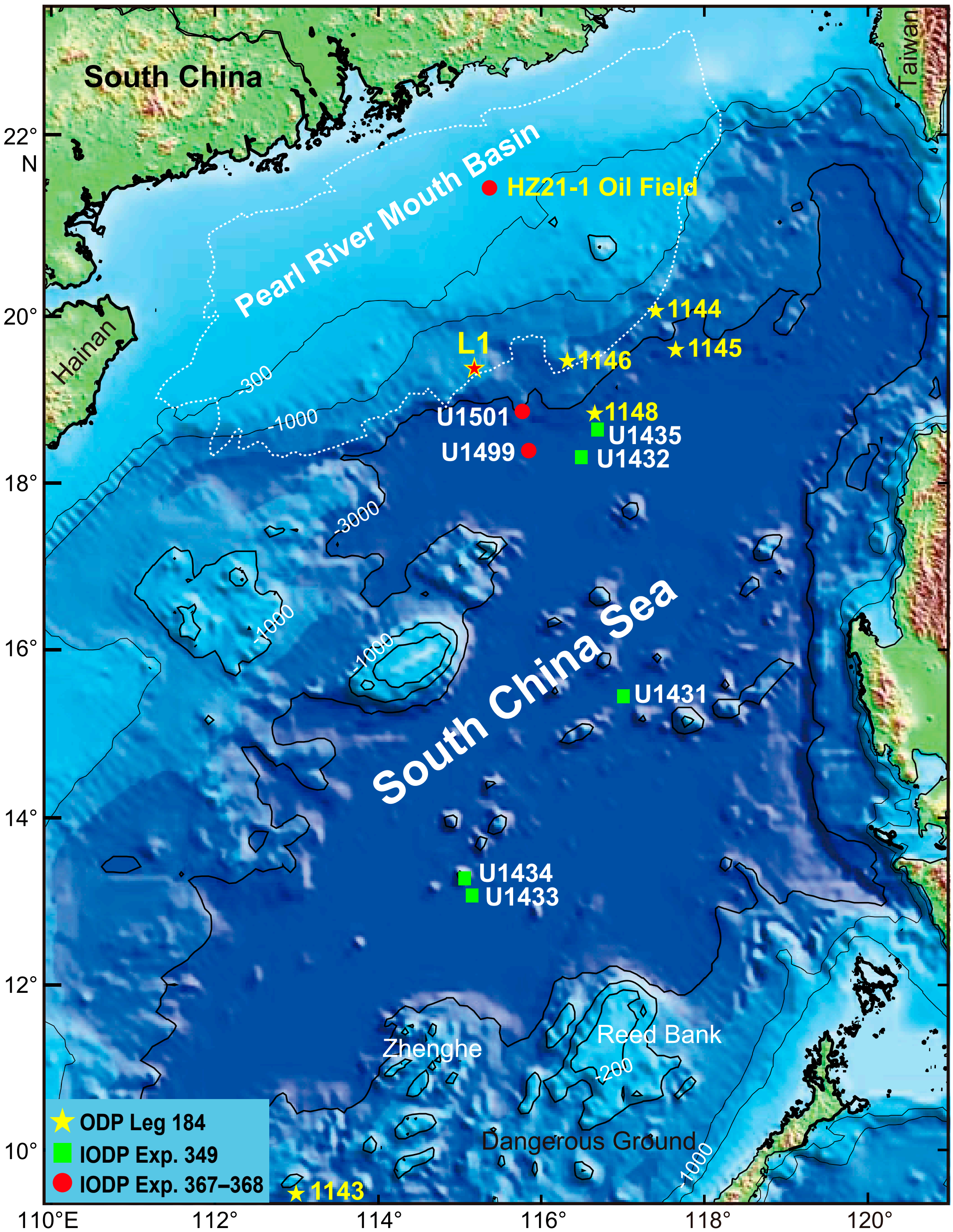

Figure 1: Bathymetric map showing the locations of the study site (L1), HZ21-1 Oil Field, and Ocean Drilling Program (ODP) and International Ocean Discovery Program (IODP) drill sites in the South China Sea (after Wang & Jiang, 2020). The dashed line represents the extent of the Pearl River Mouth Basin.

Calcareous nannofossils are one of the most valuable paleontologic tools in the oil industry due to their use in biostratigraphy, which involves correlating rock layers based on the presence, absence, and abundance changes of species, as shown by numerous studies especially in the Gulf of Mexico (e.g., Smith & Hardenbol, 1973; Denne, 2008; Olson et al., 2015; Bergen et al., 2017; De Kaenel et al., 2017; Bergen et al., 2019), North Sea (e.g., Gallagher, 1988; Thomsen et al., 2012; Vieira et al., 2020), and Middle East region (e.g., Alqudah et al., 2014; Mandur & Makled, 2016; Giraldo Gómez et al., 2017), whereas relatively few studies from the South China Sea (SCS) are published and accessible to the international community. As Akers (1986, p. 367) commented on the applications of calcareous nannofossils in the Gulf of Mexico, "Nowhere else in the world, are so many people, looking so closely, for so many key fossils, in so many drilling wells, that will produce so much oil". By analyzing fossil assemblages found in ditch cuttings or core samples obtained during oil exploration, paleontologists can establish the age of sedimentary layers, identify specific stratigraphic zones, and determine the geological history of the area. This information aids in locating potential hydrocarbon reservoirs and characterizing reservoir rocks, as well as guiding decision-making processes in drilling and exploration efforts (Akers, 1986).

This research presents a case study using material from a deep-water exploration well (L1) on the northern shelf of the SCS. This study aims to illustrate a standard protocol for applying calcareous nannofossil biostratigraphy and paleoenvironmental interpretation to hydrocarbon exploration in the region.

2. Material and methods

The studied samples are from Well L1, an exploration well drilled in 2014 by the China National Offshore Oil Corporation (CNOOC). The exploration well is located ~150 km NW of Ocean Drilling Program (ODP) Site 1148 (18°50.17'N, 116°33.94'E; 3294 m water depth) in 1921 m of water in the deepwater area of the Pearl River Mouth Basin (PRMB) on the northern slope of the SCS (Figure 1). The PRMB, a significant offshore basin located in the northern part of the SCS and well known for its high hydrocarbon potential, is characterized by diverse geological formations and sedimentary layers that are of considerable interest for oil and gas exploration activities. Its geological complexity and hydrocarbon potential have made it a focal point for various geological studies and exploration endeavors in the offshore oil industry (Sun et al., 2012; Sun et al., 2014; Mu et al., 2022; Li et al., 2023).

Drill cuttings from the studied section between 4650 and 2730 m were the only materials available for this biostratigraphic study. The cuttings are mostly dark gray to medium-dark gray calcareous silty shale. Samples for biostratigraphy were taken every 8–12 m (generally every 10 m), except between 3003 and 3000 m, which was sampled at a 3-m interval. Each sample represents a mixture of cuttings from across the spacing interval. For example, sample 2730–2740 m represents a mixture of cuttings for the 10-m interval between 2730 and 2740 m, whereas sample 3000–3003 m represents cuttings from the 3-m interval between 3000 and 3003 m. For simplicity, all samples are reported as the top depth of the sampling interval (see Table 1 for depth range of each sample). Smear slides were prepared following the modified "double slurry" method that was adapted here to process clastic rocks and cutting samples typically collected by the oil industry or from clastic settings (Watkins & Bergen, 2003; Jiang & Zhang, 2016). Samples were prepared by placing ~10 g of cuttings and mud mixture into a 30 mL plastic bottle, adding ~3 times the sample volume of deionized water buffered with NaOH (pH = 9), and then soaking the mixture for 24 h while stirring and shaking on an oscillator until completely dispersed into a suspension. Smear slides were then prepared from the mixture using the double slurry method. We used a displosable pipette to drop ~0.5 mL of the suspension onto a labeled coverslip and let it dry on a hot plate at 50˚C. After it dried, we added a small amount of ~5% sodium hexametaphosphate solution as a dispersant, which we mixed with the dried mud, and then spread it evenly on the coverslip. After it once again dried on a hot plate at 50˚C, we mounted the coverslip with Norland Optical Adhesive Number 61 and cured it with ultraviolet light.

Calcareous nannofossils were examined with a Zeiss Axio Imager A2 microscope under cross-polarized light at 1000× magnification (diameter of each field of view equal to ~0.4 mm). Photomicrographs were taken with a 6 megapixel digital camera (Zeiss Axiocam 506 color). Taxonomy primarily follows Perch-Nielsen (1985) and Bown (1998), as well as the Nannotax3 online database (Young et al., 2023). We note that Howe (2021) divided the family Sphenolithaceae into two genera based on ultrastructure, *Sphenolithus* and *Furcatolithus*, with the latter comprising the *F. predistentus-distentus-ciperoensis* lineage. However, we retain the two well-established species names *Sphenolithus predistentus* and *S. distentus* because CNOOC, for whom this study was completed, needed the taxonomy to be consistent with previous work for the zonal markers.

The zonation scheme of Martini (1971) was used with supplementary datums from Agnini et al. (2014) and Gradstein et al. (2012).

The preservation status of fossil assemblages provides information on burial and sedimentology and in this study is designated as good (G), moderate (M), or poor (P) with transitional conditions between them following Jiang & Wise (2007). For example, GM indicates a preservation

Table 1: Calcareous nannofossil datums and corresponding depths in Well L1, northern South China Sea..

Zone	Datum	Age (Ma)	Depth (m)	Confidence level
NN3/NN4	LO *Sphenolithus belemnos*	17.683	2750	***
NN2/NN3	LO *Triquetrorhabdulus carinatus*	18.28	2770	***
NN2	FO *Sphenolithus belemnos*	19.03	2890–3003	*
NN2	FO *Helicosphaera ampliaperta*	20.43	2840	*
NN2	FO *Sphenolithus disbelemnos*	22.76	3050	*
NN1	LO *Sphenolithus capricornutus*	22.97	2830	**
NN1	LO *Sphenolithus delphix*	23.11	2840	**
NP25/NN1	LO *Reticulofenestra bisecta* (>10 µm)	23.13	2840	***
NP25	LO *Zygrhablithus bijugatus*	23.76	2980	**
NP24/NP25	LO *Sphenolithus distentus*	26.84	3190	**
NP24	LO *Sphenolithus predistentus*	26.93	3190	***

Note: The nannofossil zonal definitions are based on Martini (1971) and age assignments are based on Gradstein et al. (2012). FO = first occurrence, LO = last occurrence. *Reticulofenestra bisecta* (>10 µm) corresponds to the species concept of *Reticulofenestra stavensis* according to Young et al. (2023). NN = Neogene Nannofossil, NP = Nannofossil Paleogene. Confidence level is estimated based on the following criteria: (1) a LO has the highest confidence and a FO the lowest, and (2) the distribution is continuous in the analyzed section, with barren intervals considered when defining occurrence continuity.

status that falls between good and moderate. The relative abundance of each taxon is semi-quantitatively represented according to the average number of specimens in all fields of view (FOV) encountered in a traverse as follows:

VA = very abundant (≥25 specimens per FOV).
A = abundant (6–24 specimens per FOV).
C = common (1–5 specimens per FOV).
F = few (1 specimen per 2–10 FOVs).
R = rare (1 specimen per 11–50 FOVs).
P = present (1 specimen per >50 FOVs).

To avoid missing rare species and biasing the assemblage composition during observation, at least 500 FOVs (=5 traverses) were observed. All specimens in ≥20 FOVs were counted to obtain the total abundance. If the total number was less than 400, the counting continued until 100 FOVs were reached. Total counts were then normalized to 100 FOVs (equivalent to one traverse), which was used as the total abundance of the sample.

Samples adjacent to zonal boundaries were further analyzed by examining 5 additional traverses to provide a more precise biostratigraphic determination. Only the last occurrence (LO) and/or first (continuous) occurrence (FO) of a marker species was used to define the corresponding datum, and consideration was given to barren intervals when defining the continuity of occurrence. Last occurrence datums were given higher priority considering the presence of downhole caving contamination in well cuttings. Each nannofossil datum was assigned an orbitally tuned age from Gradstein et al. (2012) to estimate linear compacted sedimentation rates. We note that Bergen et al. (2019) published orbitally tuned ages for some of the species identified in this study; however, we do not apply these ages here for two reasons. First, these ages were derived and have only been tested for the equatorial Atlantic Ocean, Gulf of Mexico, and Mediterranean Sea and additional work needs to be conducted to verify their reliability in the Pacific and Indian Oceans and the western Pacific marginal seas. Second, CNOOC, for whom this study was completed, still uses the Gradstein et al. (2012) time scale.

3. Results

Calcareous nannofossil abundance and preservation vary significantly with depth over the studied section between 4650 and 2730 m (Figures 2 and 3; Appendix 1), which allows identification of several late Oligocene–early Miocene zonal markers and allows us to divide the studied section into three intervals (Figures 2–4; Appendix 1). Selected species are illustrated in Plate 1.

Lowermost Interval I (4650–3980 m) is nearly barren with extremely low abundance and species richness. The specimens present are likely a result of downhole caving (see discussion below).

Interval II (3970–3012 m) has an abrupt increase in total abundance and species richness with improved preservation

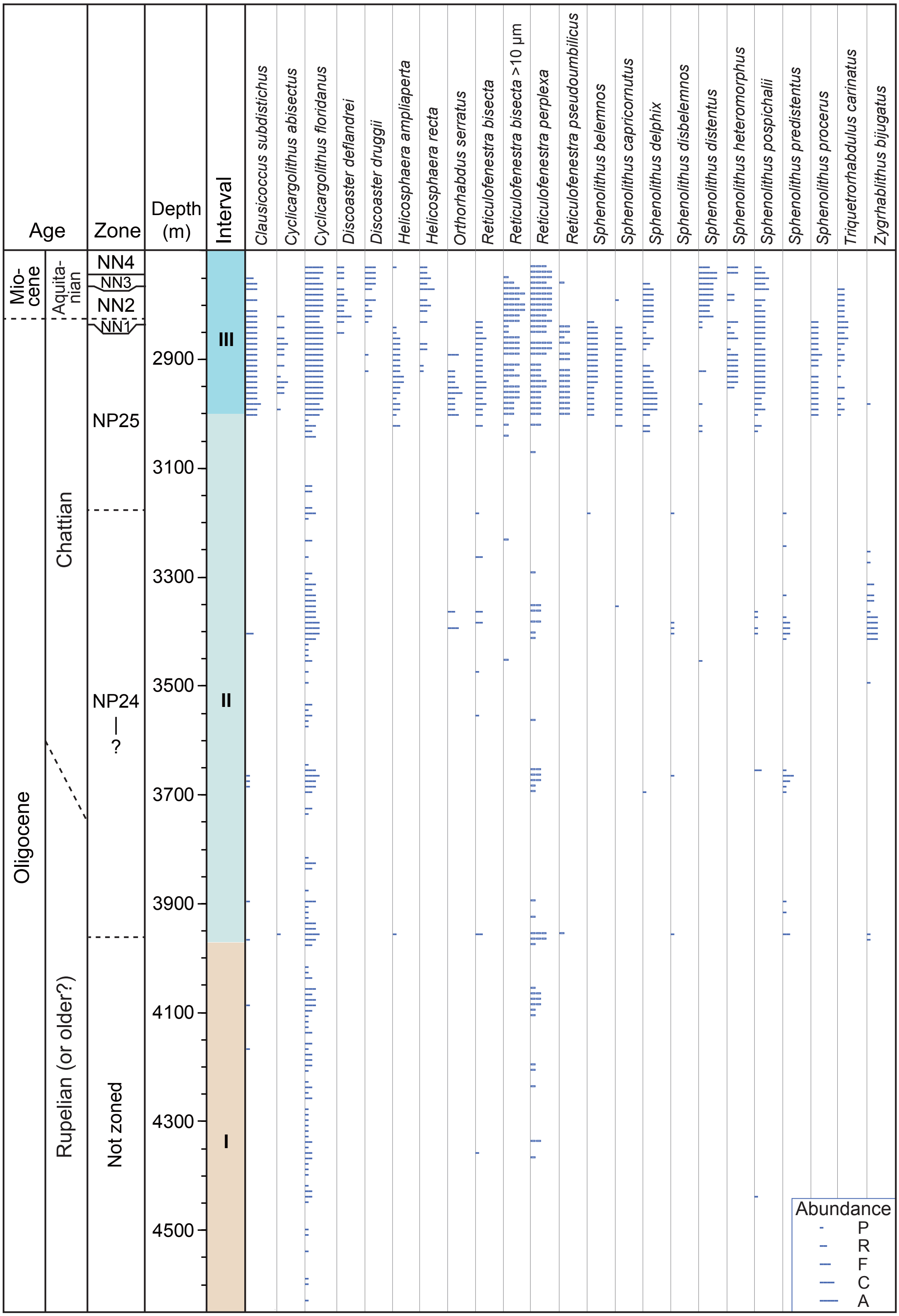

Figure 2: Distribution of selected calcareous nannofossil species from Well L1 in the Pearl River Mouth Basin, northern South China Sea

and is characterized by several small abundance peaks (e.g., in samples 3960 m, 3670 m, and 3390 m) alternating with nearly barren or barren intervals. The average abundance and species richness for these small abundance peaks are 236 (ranging from 52–902) and 11 (ranging from 6–24), respectively (Figure 3). The common taxa include various species of *Reticulofenestra*, *Cyclicargolithus floridanus*, and *Coccolithus pelagicus*, whereas *Discoaster* is very rare (Figure 2; Appendix 1). The assemblages are generally moderately to poorly preserved.

Interval III (3000–2730 m) has the highest abundance and species richness with generally moderate to moderately good preservation. The total abundance averages 7281 (range: 3975–11813), species richness averages 35 (range: 31–43), and total number of *Discoaster* specimens averages 148 (range: 7–320) (Figure 3). The most abundant taxa observed include various species of *Reticulofenestra* (e.g., *R. minuta*, *R. minutula*, *R. haqii*, and *R. pseudoumbilicus*), *Sphenolithus heteromorphus*, *Sphenolithus conicus*, *Umbilicosphaera jafari*, *C. floridanus*, *C. pelagicus*, *Discoaster deflandrei*, and *Calcidiscus leptoporus* (Figure 2; Appendix 1).

4. Discussion

4.1. Calcareous nannofossil biostratigraphy of Well L1

Oil industry wells are usually drilled in expanded continental margin sequences, where nannofossil abundance is generally low, mainly due to dilution by terrestrial clastic materials. However, the primary challenge is that samples from industry wells are often limited to ditch cuttings, which have various limitations resulting from mud contamination, downhole caving, mixed lithologies within sampled depth ranges, and inaccurate depth control.

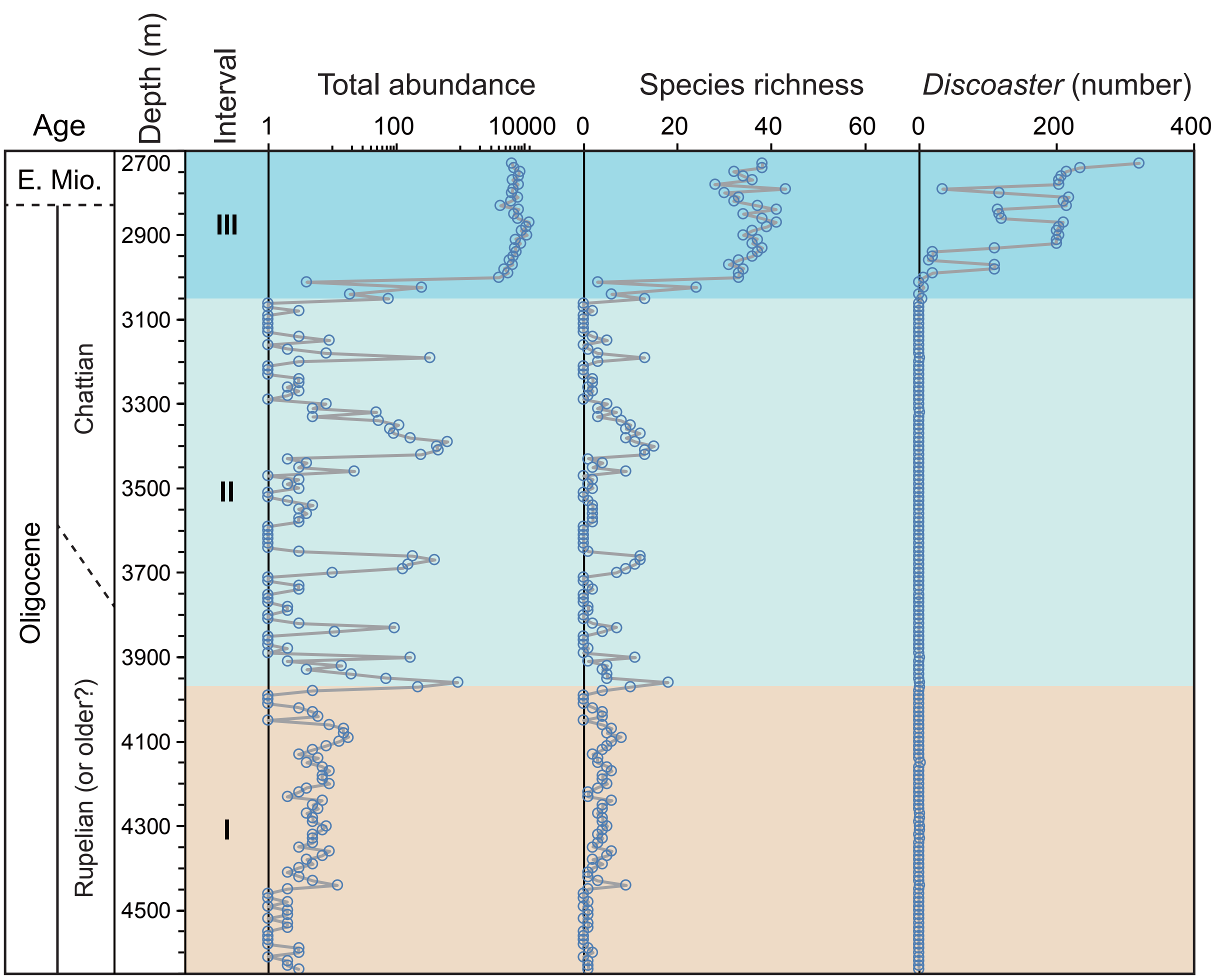

Figure 3: Paleoenvironmental evolution during the late Oligocene–Early Miocene in the Pearl River Mouth Basin interpreted from calcareous nannofossil assemblages, northern South China Sea. The paleoenvironmental interpretation is primarily based on total nannofossil abundance, species richness, and number of *Discoaster* specimens, with consideration of sedimentation rate. See text for details.

The extent of these limitations appears to relate to various aspects (e.g., drilling technologies used, drilling mud composition, cuttings washing procedures, and sampling techniques at the cuttings shaker). These challenges are particularly evident in the western PRMB compared to the eastern PRMB, where information regarding drilling operations is not always available to paleontologists. In contrast, standard practice in the Gulf of Mexico involves immediate washing and picking of rock chips for wellsite biostratigraphy, which appears to offer better results based on our own experiences working in both regions. This may explain why more datums can be used in the Gulf of Mexico region (e.g., Bergen et al., 2017, 2019).

The limitations with respect to cuttings use increase the uncertainty of biostratigraphic interpretations because the exact depth at which a specific nannofossil species was found may not be precisely known. Moreover, downhole caving and mixing can significantly deepen the FO datums and create multiple apparent FO datums (as shown in Figure 4 and Appendix 1), making it challenging to accurately identify the true FO of a nannofossil species. Therefore, when only ditch cuttings are available, generally only LO datums are used to establish the biostratigraphy, which limits the resolution of the analysis, especially for this study area.

Under such conditions, LO datums or abundance changes of calcareous nannofossil taxa not typically used for biostratigraphy can be used as a more reliable alternative to approximate a FO datum, which is a common practice to increase biostratigraphic resolution in expanded continental margin deposits when dealing with downhole contamination or other uncertainties (e.g., Duan & Huang, 1991; Huang, 1997; Denne, 2008). This approach allows for more age control and enhances the reliability and resolution of biostratigraphy in oil industry wells, in particular when dealing with intra-basin correlation as shown in the Gulf of Mexico (De Kaenel et al., 2017; Bergen et al., 2019), as well as in the study region (Duan & Huang, 1991; Huang, 1997; Jiang, 1999; Zhu & Chen, 2007). While the limitation with the use of LO datums cannot be overlooked because nannofossils are easily reworked (Romein, 1979), this is the only practical method in the oil industry to date strata from cuttings, especially in the study region where caving seems to be particularly problematic. Fortunately, reworking was not commonly observed in our samples, with only two such instances involving *Reticulofenestra bisecta* (>10 μm) and *Sphenolithus delphix* identified where their reoccurrences above a long interval of absence characterized by abundant nannofossil assemblages were considered reworked (Appendix 1). As more sophisticated and technologically advanced drilling methods are developed and utilized, the use of FO datums becomes increasingly common and reliable, as demonstrated by numerous studies originating from the Gulf of Mexico (e.g., Denne, 2007; Bergen et al., 2017; Browning et al., 2017; De Kaenel et al., 2017; Bergen et al., 2019).

Heavy downhole contamination may result in the out-of-place occurrences of certain species, such as *Sphenolithus heteromorphus* and *Helicosphaera ampliaperta*, possibly due to washing cuttings well after their initial collection or incomplete washing of cuttings because lengthy contact between drilling mud and rock chips can result in a mixed sample being taken for biostratigraphic analysis. After considering the distribution patterns of zonal markers and overall assemblages with depth (Figure 2; Appendix 1), we identified the datums of four zonal markers including *Sphenolithus distentus*, *R. bisecta* (>10 μm), *Triquetrorhabdulus carinatus*, and *Sphenolithus belemnos* (Table 1), where the positions of these datums appear reasonable considering their relative positions to other LO datums, including those of *Sphenolithus capricornutus*, *S. delphix*, *Zygrhablithus bijugatus*, and *Sphenolithus predistentus* (Table 1). This allows identification of Martini (1971) nannofossil Zones NP24–NN4 (Figure 2; Table 1; Appendix 1). Accordingly, the uppermost samples comprising mostly Interval I (2830–2730 m) are dated to the Early Miocene (from 23.0 Ma to >14.9 Ma), whereas the samples within Interval II (3970–2830 m) are tentatively assigned to the late Oligocene based on the occurrences of *R. bisecta* (>10 μm), *S. distentus*, and *S. predistentus* (Figure 2; Appendix 1). However, the deepest section, Interval III (4650–3970 m) lacks any consistently occurring age diagnostic nannofossils; therefore, no age determination can be given (Figures 2 and 4; Appendix 1).

Additional FO datums, when found to lie in reasonable positions relative to these LO datums, are also used here to provide further biostratigraphic constraints (Figure 4; Table 1). All of these datums provide a comprehensive chronological framework for exploring the paleoenvironmental conditions present in this region of the SCS during the late Oligocene and Early Miocene.

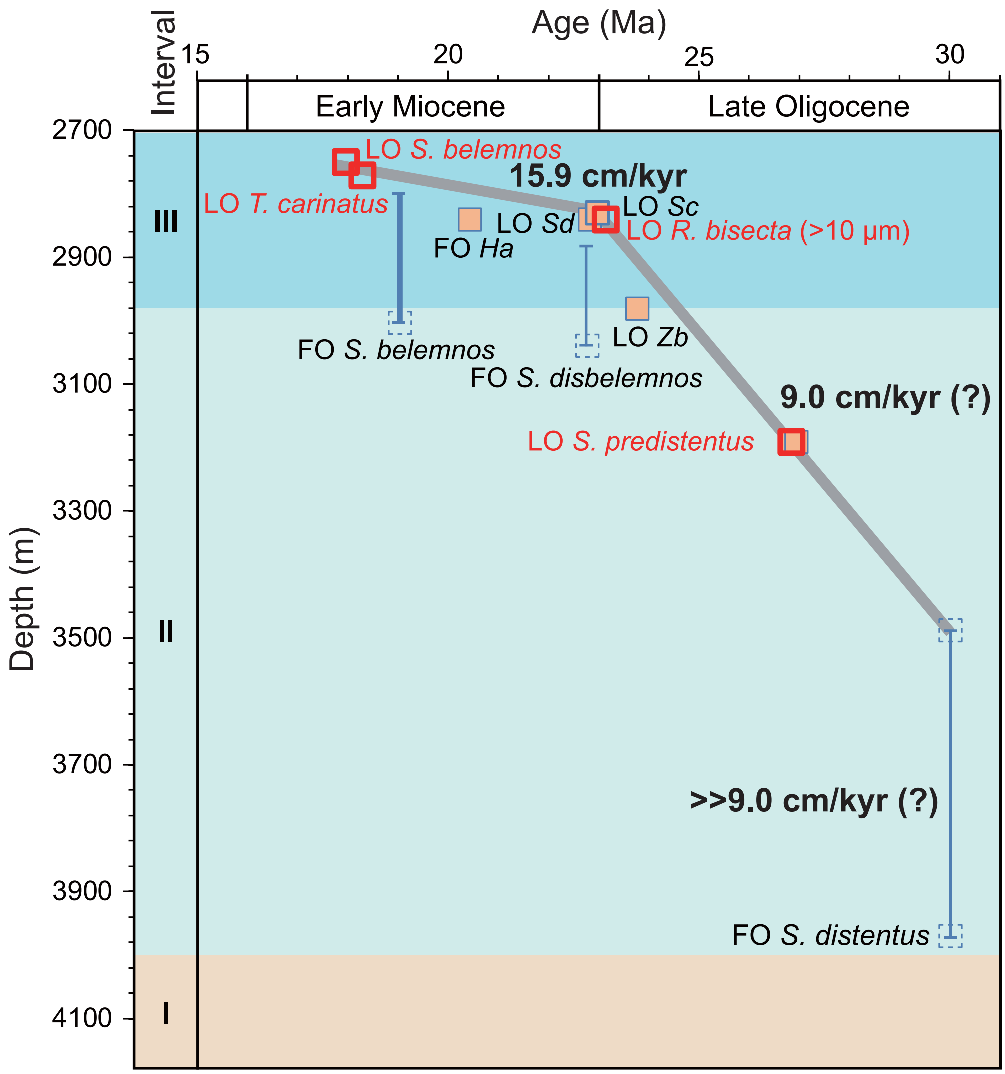

Figure 4: Age-depth plot showing variations in the sedimentation rates (cm/kyr) in Well L1 in the Pearl River Mouth Basin, northern South China Sea. Symbols with thicker, red outline indicate higher biostratigraphic confidence, whereas blue symbols with a dashed outline indicate FO datums with lower confidence levels. The oldest bioevent (FO *Sphenolithus distentus*) may be significantly deeper due to downhole contamination. If *in situ*, it suggests exceptionally high sedimentation rates. See Table 1 for the depth, age, and confidence level of each datum. FO = first occurrence; LO = last occurrence; *Sd* = *Sphenolithus delphix*; *Sc* = *Sphenolithus capricornutus*; *Ha* = *Helicosphaera ampliaperta*; *Zb* = *Zygrhablithus bijugatus*.

4.2 Environmental change during the late Oligocene–Early Miocene in the northern SCS

The SCS is a marginal basin that formed in the late Eocene (Jian et al., 2019) and has undergone continental lithosphere extensional rifting and subduction-collision processes within an overall convergent regime (Xie et al., 2022). This led to regional tectonic subsidence in the northern SCS, deepening the paleo-water depth and increasing the distance from the shoreline to the study site during the late Oligocene–Early Miocene (Wang et al., 2021). These changes are identified in seismic studies by the basin wide T60 seismic reflector (Xie et al., 2017), across which the SCS experienced rapid subsidence creating a deep-sea environment.

During the late Oligocene–Early Miocene, the Earth witnessed a period of relative global warmth interrupted by large, transient Antarctic glaciations across the boundary (Zachos et al., 2001). The paleoceanographic changes associated with the glaciations triggered variations in sea level and temperature and nutrient regimes of the upper water column (Miller et al., 2020; Westerhold et al., 2020), leading to important turnovers in calcareous nannofossil assemblages (Aubry, 1992; Bown, 2005; Plancq et al., 2013).

Microfossil distribution, abundance, and diversity data inform a variety of paleoenvironmental proxies (e.g., Culver, 1988; Mackensen et al., 1995), offering insights into water depth and sea level changes in marginal marine environment (Leckie & Olson, 2003; Galović, 2017). As commonly practiced in the Pearl River Mouth Basin of the northern SCS (Qin, 1996; Huang, 1997; Mao et al., 2019), the total nannofossil abundance, species richness, and the number of *Discoaster* specimens have been used to infer paleoenvironmental change. Specifically, *Discoaster* species are most abundant in tropical and subtropical open-ocean locations and are widely recognized as deepwater dwellers, living in warm, stratified, stable waters with a deep nutricline (Bukry, 1971; Aubry, 1998; Bralower, 2002). Conversely, the final decline in *Discoaster* abundance and its eventual extinction in the Early Pleistocene were driven by increased climate variability and nutricline shoaling (Schueth & Bralower, 2015). Therefore, we also use *Discoaster* abundance as a proxy for identifying stable, open-ocean environments in the Miocene (Figure 3).

The notable variations in the nannofossil assemblages and calculated linear sedimentation rates reflect the evolutionary history of the SCS (Figures 2–4). During Interval I (4650–3980 m) in the Oligocene prior to ~27 Ma when the SCS was shallow, the study site was likely situated very close to the shore and received large amounts of terrestrial clastic materials, resulting in high sedimentation rates (most likely >>9.0 cm/kyr; Figure 4). These environmental conditions do not favor the preservation of calcareous nannofossils and those that are preserved are subject to dilution and dissolution, resulting in a barren or near-barren nannofossil record.

Interval II (3970–3012 m) corresponds to a period characterized by alternating low abundance of nannofossils and near-barren intervals, which is indicative of an unstable environment. This alternation suggests intense tectonic activities leading to fluctuations in sea level (Shao et al., 2004; Wang et al., 2021), which is reflected by the variations in presence and absence of the coccolithophores at the study site and the high sedimentation rate (9.0 cm/kyr; Figure 4). This interval encompasses Reflector T60, which signifies widespread subsidence and landward-shifting erosion that resulted in the preservation of essentially no sedimentation across the Oligocene/Miocene boundary (Figure 4) and a widespread erosion horizon in the SCS (Pang et al., 2008; Xie et al., 2022). This accords well with the global NAq1 sea level sequence (Bergren et al., 2019).

Interval III (3000–2730 m) has the highest values in total abundance, diversity, and number of *Discoaster*, suggesting a stable, open-ocean environment and corresponding to a relatively low sedimentation rate in the Early Miocene (3.5 cm/kyr; Figure 4). This period is linked to basin-wide subsidence and increasing water depth (Pang et al., 2008; Jian et al., 2019; Wang et al., 2021; Xie et al., 2022). The timing of the environmental change to more stable conditions seems to be synchronous with the global sea level highstand during the late Oligocene (Miller et al., 2020), which could have been amplified by local tectonic subsidence and rifting (Jian et al., 2019).

5. Conclusions

We conducted a detailed calcareous nannofossil analysis on cuttings samples from the interval between 4650 and 2730 m in the hydrocarbon exploration Well L1 in the northern SCS. We identified four LO datums, as well as additional secondary datums, which allow assignment of the section to Zones NP24–NN4, dating the section to the late Oligocene–Early Miocene. Deeper than ~3200 m, the age assignment is tentative due to a paucity of nannofossils. The notable variations in the nannofossil assemblages and sedimentation rates reflect the evolutionary history of the SCS. Interval III (4650–3980 m), which is late Oligocene or older in age, is nearly barren of nannofossils with extremely low species richness but a very high sedimentation rate. This interval corresponds to a period of shallow water depths when the study site was located close to terrestrial sources, leading to high sedimentation rates and resulting in dilution of nannofossil assemblages. Interval II (3970–3012 m) is characterized by alternating intervals of low abundance with nearly barren intervals, suggesting an unstable environment due to fluctuations in sea level. This interval encompasses a period of widespread subsidence and landward-shifting erosion, resulting in little sedimentation across the Oligocene/Miocene boundary and a widespread erosion horizon in the SCS. Uppermost Interval I (3000–2739 m) is dated to the Early Miocene and has the highest total abundance, diversity, and number of *Discoaster* specimens, suggesting a stable, open-ocean environment with relatively low sedimentation rates similar to that of today.

Acknowledgements

We thank Hong Su (Jinan University) for slide preparation. Two helpful reviews by Claire Routledge and Todd Boesiger and editorial suggestions by Ines Galović and Denise Kulhanek greatly strengthened the earlier version of this manuscript. This work was funded by National Science Foundation of China (Grant Nos. 41976045, 42206047) and the Innovation Group Project of Southern Marine Science and Engineering Guangdong Laboratory (Zhuhai) (No. 311023002).

References

Agnini, C., Fornaciari, E., Raffi, I., Catanzariti, R., Palike, H., Backman, J. & Rio, D. 2014. Biozonation and biochronology of Paleogene calcareous nannofossils from low and middle latitudes. *Newsletters on Stratigraphy*, **47**(2): 131–181. https://doi.org/10.1127/0078-0421/2014/0042

Agnini, C., Monechi, S. & Raffi, I. 2017. Calcareous nannofossil biostratigraphy: historical background and application in Cenozoic chronostratigraphy. *Lethaia*, **50**(3): 447–463. https://doi.org/10.1111/let.12218

Akers, W. 1986. Calcareous nannofossils, state of the art, Gulf of Mexico: a review for oil prospectors. *Gulf Coast Association of Geological Societies Transactions*, **36**: 367–369.

Alqudah, M., Hussein, M.A., Podlaha, O.G., Den Boorn, S.V., Kolonic, S. & Mutterlose, J. 2014. Calcareous nannofossil biostratigraphy of Eocene oil shales from central Jordan. *GeoArabia*, **19**(1): 117–140. https://doi.org/10.2113/geoarabia1901117

Aubry, M.-P. 1992. Late Paleogene calcareous nannoplankton evolution: a tale of climatic deterioration. *In*: D.R. Prothero & W.A. Berggren (Eds.). *Eocene–Oligocene Climatic and Biotic Evolution*. Princeton University Press: 272–309.

Aubry, M.-P. 1998. Early Paleogene calcareous nannoplankton evolution: a tale of climatic amelioration. *In*: M.-P. Aubry, S.G. Lucas & W.A. Berggren (Eds.). *Late Paleocene and Early Eocene Climatic and Biotic Events in the Marine and Terrestrial Records*. Columbia University Press: 158–203.

Backman, J., Raffi, I., Rio, D., Fornaciari, E. & Pälike, H. 2012. Biozonation and biochronology of Miocene through Pleistocene calcareous nannofossils from low and middle latitudes. *Newsletters on Stratigraphy*, **45**(3): 221–244. https://doi.org/10.1127/0078-0421/2012/0022

Bergen, J.A., Kaenel, E.D., Blair, S.A., Boesiger, T.M. & Browning, E. 2017. Oligocene–Pliocene taxonomy and stratigraphy of the genus *Sphenolithus* in the circum North Atlantic Basin: Gulf of Mexico and ODP Leg 154. *Journal of Nannoplankton Research*, **37**(2–3): 77–112. https://doi.org/10.58998/jnr2016

Bergen, J.A., Truax, S., Iii, De Kaenel, E., Blair, S., Browning, E., Lundquist, J., Boesiger, T., Bolivar, M. & Clark, K. 2019. BP Gulf of Mexico Neogene Astronomically-tuned Time Scale (BP GNATTS). *GSA Bulletin*, **131**(11–12): 1871–1888. https://doi.org/10.1130/B35062.1

Billard, C. & Inouye, I. 2004. What is new in coccolithophore biology? *In*: H.R. Thierstein & J.R. Young (Eds.). *Coccolithophores – From molecular processes to global impact*. Springer, Berlin: 1–29.

Bown, P.R. 1998. *Calcareous nannofossil biostratigraphy*. British Micropaleontological Society Publications Series. Chapman & Hall, London: 315pp.

Bown, P.R. 2005. Calcareous nannoplankton evolution: a tale of two oceans. *Micropaleontology*, **51**(4): 299–308. https://doi.org/10.2113/gsmicropal.51.4.299

Bralower, T.J. 2002. Evidence of surface water oligotrophy during the Paleocene–Eocene thermal maximum; nannofossil assemblage data from Ocean Drilling Program Site 690, Maud Rise, Weddell Sea. *Paleoceanography*, **17**(2): 13-1–13-12. https://doi.org/10.1029/2001PA000662

Browning, E.L., Bergen, J.A., Blair, S.A., Boesiger, T.M. & De Kaenel, E. 2017. Late Miocene to Late Pliocene taxonomy and stratigraphy of the genus *Discoaster* in the circum North Atlantic Basin: Gulf of Mexico and ODP Leg 154. *Journal of Nannoplankton Research*, **37**(2–3): 189–214. https://doi.org/10.58998/jnr2037

Bukry, D. 1971. Discoaster evolutionary trends. *Micropaleontology*, **17**(1): 43–52. https://doi.org/10.2307/1485036

Culver, S.J. 1988. New foraminiferal depth zonation of the northwestern Gulf of Mexico. *Palaios*, **3**(1): 69–85. https://doi.org/10.2307/3514545

De Kaenel, E., Bergen, J.A., Browning, E.L., Blair, S.A. & Boesiger, T.M. 2017. Uppermost Oligocene to Middle Miocene Discoaster and Catinaster taxonomy and stratigraphy in the circum North Atlantic Basin: Gulf of Mexico and ODP Leg 154. *Journal of Nannoplankton Research*, **37**(2–3): 215–244. https://doi.org/10.58998/jnr2077

De Vargas, C., Aubry, M.-P., Probert, I. & Young, J.R. 2007. Origin and evolution of coccolithophores: From coastal hunters to oceanic farmers. *In*: P.G. Falkowski & A.H. Knoll (Eds.). *Evolution of Primary Producers in the Sea*. Academic Press: 251–285. https://doi.org/10.1016/B978-012370518-1/50013-8

Denne, R.A. 2007. Paleogene calcareous nannofossil bioevents from the fold belts of the deep-water central Gulf of Mexico. *In*: L. Kennan, J. Pindell & N.C. Rosen (Eds.). *27th GCSSEPM Foundation Annual Bob F. Perkins Research Conference Proceedings: The Paleogene of the Gulf of Mexico and Caribbean Basins: Processes, Events, and Petroleum Systems*: 211–231. https://doi.org/10.5724/gcs.07.27.0211

Denne, R.A. 2008. Utilizing abundance changes of new and non-standard calcareous nannofossil taxa to increase biostratigraphic resolution in expanded continental margin deposits: Examples from the Middle and Lower Miocene of the Gulf of Mexico. *Gulf Coast Association of Geological Societies Transactions*, **58**: 227–239.

Duan, W. & Huang, Y. 1991. Tertiary calcareous nannofossil biostratigraphy in the north part of the South China Sea. *Acta Geologica Sinica (English Edition)*, **4**(3): 321–339. https://doi.org/10.1111/j.1755-6724.1991.mp4003008.x

Gallagher, L.T. 1988. *Tertiary calcareous nannofossils from the central and southern North Sea Basins, and their biostratigraphical application*. PhD thesis, University of London: 492pp.

Galović, I. 2017. Sarmatian calcareous nannofossil assemblages in the SW Paratethyan marginal marine environments: Implications for palaeoceanography and the palaeoclimate. *Progress in Oceanography*, **156**: 209–220. https://doi.org/10.1016/j.pocean.2017.05.011

Giraldo Gómez, V.M., Beik, I., Podlaha, O.G. & Mutterlose, J. 2017. The micropaleontological record of marine early Eocene oil shales from Jordan. *Palaeogeography, Palaeoclimatology, Palaeoecology*, **485**: 723–739. https://doi.org/10.1016/j.palaeo.2017.07.030

Gradstein, F.M., Ogg, J.G. & Schmitz, M. 2012. *The Geologic Time Scale 2012, Volume 1*. Elsevier: 1144pp.

Haq, B.U. 1983. *Calcareous nannoplankton.* Benchmark Papers in Geology, 79. Hutchinson Ross: 338 pp.

Howe, R. 2021. Ultrastructure and taxonomy of the family Sphenolithaceae. *Journal of Nannoplankton Research*, **39**(1): 29–75. https://doi.org/10.58998/jnr2124

Huang, L.S. 1997. Calcareous nannofossil biostratigraphy in the Pearl River Mouth Basin, South China Sea, and Neogene reticulofenestrid coccoliths size distribution pattern. *Marine Micropaleontology*, **32**(1–2): 31–57. https://doi.org/10.1016/S0377-8398(97)00012-1

Jian, Z., Jin, H., Kaminski, M.A., Ferreira, F., Li, B. & Yu, P.S. 2019. Discovery of the marine Eocene in the northern South China Sea. *National Science Review*, **6**(5): 881–886. https://doi.org/10.1093/nsr/nwz084

Jiang, S. 1999. High resolution calcareous nannofossil biostratigraphy and sequence stratigraphy of Well PY27-2-1, Pearl River Mouth Basin. *China Offshore Oil and Gas (Geology)*, **13**(3): 189–195.

Jiang, S. & Wise, S.W., Jr. 2007. Upper Cenozoic calcareous nannofossil biostratigraphy and inferred sedimentation, ODP Leg 206, East Pacific Rise. *Proceedings of the Ocean Drilling Program*, *Scientific Results*, **206**: 1–25. https://doi.org/10.2973/odp.proc.sr.206.008.2007

Jiang, S. & Zhang, A. 2016. A slide-making technique for preparing calcareous nannofossils from large amount of samples. *Acta Micropalaeontologica Sinica*, **33**(2): 207–210. (In Chinese with English abstract.)

Leckie, M. & Olson, H. 2003. Foraminifera as proxies for sea-level change on siliciclastic margins. *In*: H. Olson & M. Leckie (Eds.). *Micropaleontologic Proxies for Sea-Level Change and Stratigraphic Discontinuities*. SEPM Society for Sedimentary Geology: 5–19. https://doi.org/10.2110/pec.03.75.0005

Li, G., Mei, L., Ye, Q., Pang, X., Zheng, J. & Li, W. 2023. Post-rift faulting controlled by different geodynamics in the Pearl River Mouth Basin, northern South China Sea margin. *Earth-Science Reviews*, **237**: 104311. https://doi.org/10.1016/j.earscirev.2022.104311

Mackensen, A., Schmiedl, G., Harloff, J. & Giese, M. 1995. Deep-sea foraminifera in the South Atlantic Ocean: Ecology and assemblage generation. *Micropaleontology*, **41**(4): 342–358. https://doi.org/10.2307/1485808

Mandur, M.M.M. & Makled, W.A. 2016. Implications of calcareous nannoplankton biostratigraphy and biochronology of the Middle–Late Miocene of the Nile Delta, Egypt. *Arabian Journal of Geosciences*, **9**(3): 203. https://doi.org/10.1007/s12517-015-2032-z

Mao, X., Xu, S. & Liu, X. 2019. Late Cenozoic high resolution bio-stratigraphy and its bearing on sea-level fluctuation in the western Pearl River Mouth Basin. *Marine Geology & Quaternary Geology*, **39**(3): 40–50.

Martini, E. 1971. Standard Tertiary and Quaternary calcareous nannoplankton zonation. *In*: A. Farinacci (Ed.). *Proceedings of the II Planktonic Conference*. Edizioni Tecnoscienza: 739–785.

Miller, K.G., Browning, J.V., Schmelz, W.J., Kopp, R.E., Mountain, G.S. & Wright, J.D. 2020. Cenozoic sea-level and cryospheric evolution from deep-sea geochemical and continental margin records. *Science Advances,* **6**(20):

eaaz1346. https://doi.org/10.1126/sciadv.aaz1346

Mu, D., Peng, G., Zhu, D., Li, S., Suo, Y., Zhan, H. & Zhao, L. 2022. Structure and formation mechanism of the Pearl River Mouth Basin: Insights from multi-phase strike-slip motions in the Yangjiang Sag, SE China. *Journal of Asian Earth Sciences*, **226**: 105081. https://doi.org/10.1016/j.jseaes.2022.105081

Mutterlose, J., Bornemann, A. & Herrle, J. 2005. Mesozoic calcareous nannofossils — state of the art. *Paläontologische Zeitschrift*, **79**(1): 113–133. https://doi.org/10.1007/BF03021757

Olson, H.C., Snedden, J.W. & Cunningham, R. 2015. Development and application of a robust chronostratigraphic framework in Gulf of Mexico Mesozoic exploration. *Interpretation*, **3**(2): SN39–SN58. https://doi.org/10.1190/INT-2014-0179.1

Pang, X., Chen, C., Peng, D., Zhou, D., Shao, L., He, M. & Liu, B. 2008. Basic geology of Baiyun deep-water area in the northern South China Sea. *China Offshore Oil Gas*, **20**(4): 215–222.

Perch-Nielsen, K. 1985. Cenozoic calcareous nannofossils. *In*: H.M. Bolli, J.B. Saunders & K. Perch-Nielsen (Eds.). *Plankton Stratigraphy*. Cambridge University Press: 427–554.

Plancq, J., Mattioli, E., Henderiks, J. & Grossi, V. 2013. Global shifts in Noelaerhabdaceae assemblages during the late Oligocene–early Miocene. *Marine Micropaleontology*, **103**: 40–50. https://doi.org/10.1016/j.marmicro.2013.07.004

Qin, G. 1996. Application of micropaleontology to the sequence stratigraphic studies of Late Cenozoic in the Zhujiang River Mouth Basin. *Marine Geology and Quaternary Geology*, **16**(4): 17–23.

Romein, A.J.T. 1979. Lineages in early Paleogene calcareous nannoplankton. *Utrecht Micropaleontological Bulletins*, **22**: 230pp.

Rost, B. & Riebesell, U. 2004. Coccolithophores and the biological pump: responses to environmental changes. In: H.R. Thierstein & J.R. Young (Eds). *Coccolithophores – From Molecular Process to Global Impact*. Springer, Berlin: 99–125.

Schueth, J.D. & Bralower, T.J. 2015. The relationship between environmental change and the extinction of the nannoplankton *Discoaster* in the early Pleistocene. *Paleoceanography*, **30**(7): 863–876. https://doi.org/10.1002/2015PA002803

Shao, L., Li, X. & Wang, P. 2004. Sedimentary record of the tectonic evolution of the South China Sea since the Oligocene—Evidence from deep sea sediments of ODP Site 1148. *Advances in Earth Science*, **19**(4): 539–544.

Smith, L.A. & Hardenbol, J. 1973. Calcareous nannofossil applications in the Gulf of Mexico-Caribbean region. *Gulf Coast Association of Geological Societies Transactions*, **23**: 427–431.

Sun, Q., Wu, S., Cartwright, J. & Dong, D. 2012. Shallow gas and focused fluid flow systems in the Pearl River Mouth Basin, northern South China Sea. *Marine Geology*, **315–318**: 1–14. https://doi.org/10.1016/j.margeo.2012.05.003

Sun, Z., Xu, Z., Sun, L., Pang, X., Yan, C., Li, Y., Zhao, Z., Wang, Z. & Zhang, C. 2014. The mechanism of post-rift fault activities in Baiyun sag, Pearl River Mouth basin. *Journal of Asian Earth Sciences*, **89**: 76–87. https://doi.org/10.1016/j.jseaes.2014.02.018

Taylor, A.R., Brownlee, C. & Wheeler, G. 2017. Coccolithophore Cell Biology: Chalking Up Progress. *Annual Review of Marine Science*, **9**(1): 283–310.

Thomsen, E., Abrahamsen, N., Heilmann-Clausen, C., King, C. & Nielsen, O.B. 2012. Middle Eocene to earliest Oligocene development in the eastern North Sea Basin: Biostratigraphy, magnetostratigraphy and palaeoenvironment of the Kysing-4 borehole, Denmark. *Palaeogeography, Palaeoclimatology, Palaeoecology*, **350**: 212–235. https://doi.org/10.1016/j.palaeo.2012.06.034

Vieira, M., Mahdi, S. & Holmes, N. 2020. High resolution biostratigraphic zonation for the UK central North Sea Paleocene. *Marine and Petroleum Geology*, **117**: 104400. https://doi.org/10.1016/j.marpetgeo.2020.104400

Wang, Y. & Jiang, S. 2020. Variation in middle–late Miocene sedimentation rates in the northern South China Sea and its regional geological implications. *Marine Micropaleontology*, **160**: 101911. https://doi.org/10.1016/j.marmicro.2020.101911

Wang, Y., Jin, H., Jian, Z. & Xu, J. 2021. The response of paleo-water depth to T60 tectonic movement in the northern South China Sea during the late Oligocene to early Miocene. *Haiyang Xuebao*, **43**(5): 79–87.

Watkins, D.K. & Bergen, J.A. 2003. Late Albian adaptive radiation in the calcareous nannofossil genus *Eiffellithus*. *Micropaleontology*, **49**(3): 231–251. https://doi.org/10.2113/49.3.231

Westerhold, T., Marwan, N., Drury, A.J., Liebrand, D., Agnini, C., Anagnostou, E., Barnet, J.S.K., Bohaty, S.M., De Vleeschouwer, D., Florindo, F., Frederichs, T., Hodell, D.A., Holbourn, A.E., Kroon, D., Lauretano, V., Littler, K., Lourens, L.J., Lyle, M., Pälike, H., Röhl, U., Tian, J., Wilkens, R.H., Wilson, P.A. & Zachos, J.C. 2020. An astronomically dated record of Earth's climate and its predictability over the last 66 million years. *Science*, **369**: 1383–1387. https://doi.org/10.1126/science.aba6853

Winter, A. & Siesser, W.G. 1994. *Coccolithophores*. Cambridge University Press: 252pp.

Xie, X., Zhao, S., Ren, J., Yang, Y. & Yao, Y. 2022. Marginal sea closure process and genetic mechanism of South China Sea during post-spreading period. *Earth Science*, **47**(10): 3524–3542.

Xie, Z., Sun, L., Pang, X., Zheng, J. & Sun, Z. 2017. Origin of the Dongsha Event in the South China Sea. *Marine Geophysical Research*, **38**(4): 357–371. https://doi.org/10.1007/s11001-017-9321-8

Young, J., Bown, P. & Lees, J. 2017. Nannotax3 website. International Nannoplankton Association. Accessed: 3 March 2023. URL: http://www.mikrotax.org/Nannotax3.

Young, J.R., Geisen, M. & Probert, I. 2005. A review of selected aspects of coccolithophore biology with implications for paleobiodiversity estimation. *Micropaleontology*, **51**(4): 267–288. https://doi.org/10.2113/gsmicropal.51.4.267

Zachos, J., Pagani, M., Sloan, L., Thomas, E. & Billups, K. 2001. Trends, rhythms, and aberrations in global climate 65 Ma to present. *Science,* **292**(5517): 686–693. https://doi.org/10.1126/science.1059412

Zhu, Y. & Chen, F. 2007. Review of the Neogene calcareous nannofossil research of the Pearl River Mouth basin, South China. *Acta Micropalaeontologica Sinica*, **24**(1): 76–81.

Plate 1

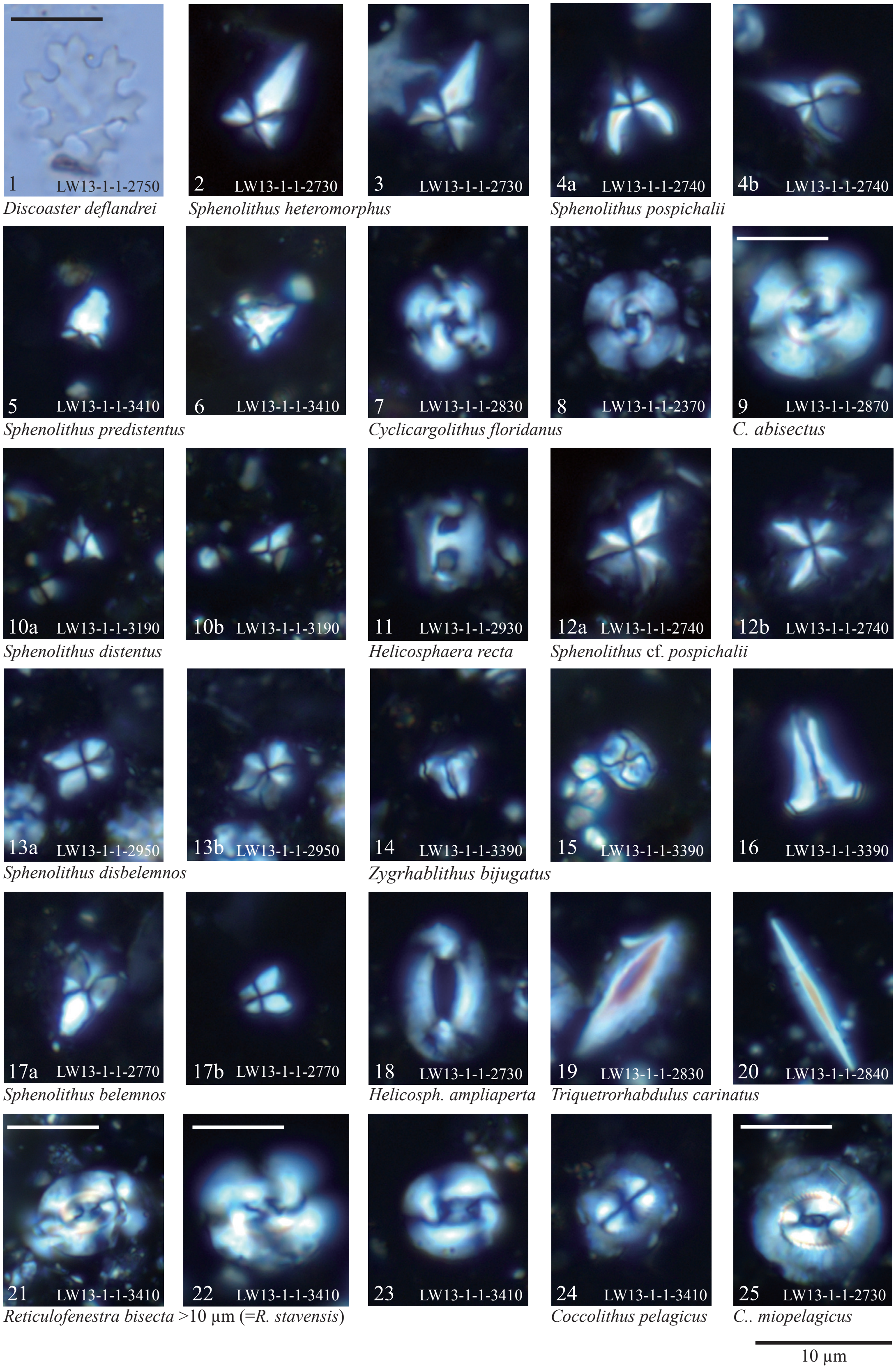

Plate 1: Calcareous nannofossil distribution in Well L1, northern South China Sea.

Age	Zone	Interval	Sample depth (m)	Total abundance (100 FOVs)	Species richness	Number of *Discoaster* specimens	Preservation	*Blackites* sp.	*Calcidiscus leptoporus*	*Calcidiscus macintyrei*	*Calcidiscus premacintyrei*	*Calcidiscus tropicus*	*Clausicoccus subdistichus*	*Coccolithus miopelagicus*	*Coccolithus pelagicus*	*Coronocyclus nitescens*	*Cyclicargolithus abisectus*	*Cyclicargolithus floridanus*	*Discoaster challengeri*	*Discoaster deflandrei*	*Discoaster druggii*	*Discoaster exilis*	*Discoaster moorei*	*Discoaster petaliformis*	*Discoaster signus*	*Discoaster* sp. (5 rays)	*Discoaster* sp. (6 rays)	*Discoaster variabilis*	*Hayaster perplexus*
Miocene Aquitanian	NN4	III	2730-2740	6310	38	320	M	R	C			F		R	C	F		A		C	R	R	R	F	C		C		R
			2740-2750	6772	38	234	M		C			F		R	C	F		A		C	R	R	R	P	F	F	C	R	R
	NN3		2750-2760	8434	32	214	M		C		R	F	R	P	C	R		C		C	R					F	C		
			2760-2770	7994	34	207	M	R	C			F	F	P	C	R		A		C			R			R	C		
	NN2		2770-2780	6557	36	204	MG		F			R	F		C	R		A	P	C	R						C		
			2780-2790	7960	28	204	M		F			R			C	F		A		C	R						C		
			2790-2800	6586	43	34	MG	R	F			R	F	P	C	F		A	R	F	F					R	F		
			2800-2810	6336	30	117	M		F			R			C	F		A		C	R					R	F		
			2810-2820	7883	33	218	MG		F			F	F		C	R		A		C	R		R				C	F	
			2820-2830	6206	32	210	MG		F			F	F		A	F	R	C	P	C	C						F		R
	NN1		2830-2840	4233	37	214	M		F	P		F	F		C	F		C		C	R						C	F	
Oligocene Chattian	NP25		2840-2850	8106	41	114	M		F			F	F		C	R	R	A		C							F	R	R
			2850-2860	6842	34	117	M		F			F	F		C			A		C	R						F	R	
			2860-2870	7858	38	120	MG		C		P	F	F	P	A		R	A	R	C							F	F	
			2870-2880	11813	41	210	M		F	R	F	F	F	R	C	F	F	A		C							C	F	
			2880-2890	10503	39	204	M		C		P	F	F	R	C	P	R	A		C							C	R	
			2890-2900	8886	36	200	MG		C			R	F		C	R	R	A		C							C		
			2900-2910	10820	34	204	M		F			F	F		A			A		C			R				C		
			2910-2920	7304	37	200	M		F			F	F		A	R	R	A		C							C		
			2920-2930	8626	36	200	M		F			F	F		A			A		C							C		
			2930-2940	7106	38	110	M		F			F	F		C	R	P	A		F							C		
			2940-2950	7491	37	20	M		F			F	F		C	R	F	A		F							F		
			2950-2960	6630	36	20	M		R			R	F		C		R	A		F							F		
			2960-2970	5782	33	14	MP		R				F		C	R	R	A		R							F		
			2970-2980	6486	31	110	MP		R		P		F		C			A		F							C		
			2980-2990	4824	34	110	M		R			P	C		C	R		C		F							C		
			2990-3000	5557	33	20	M		P				F	P	F	R	P	A		F							F		
			3000-3003	3975	33	7	MP		R				F		C	R		C		R							R		
		II	3012-3015	3	3	0	M											P											
			3024-3027	248	24	7	MP		R						F			F		R							R		
			3040-3050	18	6	0	MP								R			R											
			3050-3056	74	13	4	MP		R						R			F									R		
			3062-3065	0	0	0		BARREN																					
			3071-3080	0	0	0		BARREN																					
			3080-3090	2	2	0	MP								P														
			3090-3100	0	0	0		BARREN																					
			3100-3110	0	0	0		BARREN																					
			3110-3120	0	0	0		BARREN																					
			3120-3130	0	0	0		BARREN																					
			3130-3140	0	0	0		BARREN																					
			3140-3150	2	2	0	P								P			R											
			3150-3160	8	5	0	P											R											
			3160-3170	0	0	0																							
			3170-3180	1	1	0	MP																						
			3180-3190	7	3	0	MP											R											
	NP24 — ?		3190-3200	330	13	1	MP								F			F		P									
			3200-3210	2	3	0	MP								P			P											
			3210-3220	0	0	0		BARREN																					
			3220-3230	0	0	0		BARREN																					
			3230-3240	0	0	0		BARREN																					
			3240-3250	2	2	0	M											R											
			3250-3260	2	2	0	MP																						
			3260-3270	1	1	0	MP																						
			3270-3280	2	2	0	M											P											
			3280-3290	1	1	0	MP																						
			3290-3300	0	0	0		BARREN																					
			3300-3310	7	5	0	MP											R											
			3310-3320	4	3	0	MP											P											
			3320-3330	48	7	1	MP								R			F									P		
			3330-3340	4	3	0	MP								P			R											
			3340-3350	52	8	0	MP								R			F											
			3350-3360	108	10	0	MP								R			F											
			3360-3370	78	9	0	MP								R			F											
			3370-3380	90	12	0	MP								R			F											

Sample depth (m)	***Helicosphaera ampliaperta***	*Helicosphaera carteri*	*Helicosphaera euphratis*	*Helicosphaera obliqua*	*Helicosphaera recta*	*Helicosphaera* sp.	*Hughesius tasmaniae*	*Orthorhabdus serratus*	*Pontosphaera multipora*	*Pyrocyclus orangensis*	*Reticulofenestra ampla*	*Reticulofenestra bisecta*	***Reticulofenestra bisecta* (>10 μm)**	*Reticulofenestra bisecta filewiczii*	*Reticulofenestra haqii*	*Reticulofenestra lockeri*	*Reticulofenestra minuta*	*Reticulofenestra minutula*	*Reticulofenestra perplexa*	*Reticulofenestra pseudoumbilicus*
2730-2740	F	C	R	R	P			R	R		C				C		A	A		F
2740-2750	F	C	R	R				R	R		C				C	F	VA	A		C
2750-2760	F	C	R	R			F	F	F		C				C	F	VA	C		C
2760-2770	F	C	F	R				R	F		F		P		C	F	VA	A		F
2770-2780	R	F	R	F		R	R	C	R		C				C	F	VA	C		C
2780-2790		C	R	R					F		C				C	F	VA	C		C
2790-2800	F	C	F	R			R	R	F		F				C	F	A	C		C
2800-2810	P	F	P					F	F	R	F				C		A	C		C
2810-2820	R	F	F				R	R	F		C				C		VA	C		C
2820-2830	R	F	F				F		F		C				C	R	A	C		F
2830-2840	P	C	R	R				R	R		C				F		A	C	R	C
2840-2850		F	F	R	P	F	P		F		C		**R**		A	F	A	A	R	F
2850-2860		F	F		P	R	R		F		C		R		A		A	A	R	F
2860-2870		F	F	R	R	F			F	R	C		P		A	R	A	A	F	
2870-2880		F	F	R	R	R	R	R	F		C		R		A	R	VA	A	R	C
2880-2890		F	F	R	R	F	F	R	R		C				A	R	VA	A	R	C
2890-2900	P	F	F	R	R		P		R		F	F	R		A	R	VA	A	R	F
2900-2910		F	F	F	R		C		F		F		R		A	R	VA	A	R	
2910-2920		F	F	F	R	R	C	P	F		F				A	R	VA	A	R	R
2920-2930	P	F	F		R	R	F	P	R		F	R	R		C	R	VA	C	R	R
2930-2940		F	F	R	F	F	F		R		F	R	R		C	F	VA	A	R	R
2940-2950		F	F	R	F	F	F		R	R	F	R	R		C	F	VA	A	F	F
2950-2960		F	P		R	R	F		R		F	F	R		C	R	VA	C	F	F
2960-2970		R	P		R	R	F		R		R	C	R		C	F	VA	C	R	R
2970-2980		R	R		P	R	F				F	R	R		A		VA	C	R	R
2980-2990		R	R		R		F		R			R	R		C	R	VA	C	F	R
2990-3000		R	R		R		F		R			R	R		F	P	VA	C	R	R
3000-3003		P	R		P	R	R				R	F	R		R	R	A	C	R	R
3012-3015															R					
3024-3027			R	P	R		R		P							R	F	F	R	R
3040-3050																				
3050-3056			P			R					R				R		R	R		
3062-3065	BARREN																			
3071-3080	BARREN																			
3080-3090																				P
3090-3100	BARREN																			
3100-3110	BARREN																			
3110-3120	BARREN																			
3120-3130	BARREN																			
3130-3140	BARREN																			
3140-3150																				
3150-3160															P		R	R		
3160-3170																				
3170-3180																				
3180-3190															P					
3190-3200															F	R	F	F	P	
3200-3210																				
3210-3220	BARREN																			
3220-3230	BARREN																			
3230-3240	BARREN																			
3240-3250																				
3250-3260																				
3260-3270																				
3270-3280																			R	
3280-3290																				
3290-3300	BARREN																			
3300-3310															P			P		P
3310-3320															P	P				
3320-3330																P		R		
3330-3340																				
3340-3350																P	R	R		
3350-3360									P		R					P	F	R		
3360-3370											R				R			R		R
3370-3380			P								P	R				R		R	R	R

Sample depth (m)	*Rhabdosphaera* sp.	***Sphenolithus belemnos***	*Sphenolithus calyculus*	*Sphenolithus capricornutus*	*Sphenolithus conicus*	***Sphenolithus delphix***	*Sphenolithus disbelemnos*	*Sphenolithus dissimilis*	***Sphenolithus distentus***	*Sphenolithus heteromorphus*	*Sphenolithus pospichalii*	*Sphenolithus moriformis*	***Sphenolithus predistentus***	*Sphenolithus procerus*	*Sphenolithus* sp.	***Triquetrorhabdulus carinatus***	*Triquetrorhabdulus milowii*	*Umbilicosphaera jafari*	*Umbilicosphaera rotula*	***Zygrhablithus bijugatus***
2730-2740	R				F					F	F	R			C		R	A	F	
2740-2750	P				F					A	F	F			C		R	C	F	
2750-2760		**P**			F					A		C			C			C	F	
2760-2770		R			C		R			C		F			C		R	A	C	
2770-2780	R	F			F		F			C		C			C	**R**	R	A	F	
2780-2790		C			C		F			C	R				C	R	R	A	R	
2790-2800	R	F			C	P	F			C	R	F			C	R	F	C	F	
2800-2810		C			C		F			F		R			C	R	R	C	F	
2810-2820		C			C		F			F		F			C	R	P	C	F	
2820-2830		F			C		F			C		F			C	R		C	F	
2830-2840		F		R	F		F	F		P	F	F		R	C	F	R	C	R	
2840-2850		P		F	C	**R**	P	R		P	P	F		R	C	F	R	C	F	
2850-2860		P		F	C	R	P				R	F		R	C	R	R	C	F	
2860-2870		F		F	A	R	F				F	F		R	C	F		C	F	
2870-2880		F		F	C	R	R					R		R	C	R		C	F	
2880-2890		F		F	C	F	P				P	F		R	C	P		C	F	
2890-2900		F		F	C	R					F	F		F	C	R		C	F	
2900-2910				F	C	R		R			F	F		R	C	R	R	C	F	
2910-2920		F		F	C	R	R				F	F		R	C	P	R	C	F	
2920-2930		R		F	C	R	F	R		R	F	F			C			F	R	
2930-2940		F		F	C	R	R				F	F		R	C	P	R	F	F	
2940-2950		P		F	C	R	F				F	F		R	C			F	F	
2950-2960		F		R	C	R	F				R	F		R	C	R	P	F	R	
2960-2970		F		R	C	R	C					F		R	C			F	R	
2970-2980		F		R	C	R	C					R		R	C	R		F	R	
2980-2990		R		R	C	R	C			P		R		R	C	P		F	R	**P**
2990-3000		R		R	C	R	C					F		R	C	R		F	R	
3000-3003		R	R	R	C	R	R					P		R	C	P		F	R	
3012-3015															P					
3024-3027		P			R	R	R			P		R			F			F	R	
3040-3050							R			P		P			R					
3050-3056		P			P										R					
3062-3065	BARREN																			
3071-3080	BARREN																			
3080-3090																				
3090-3100	BARREN																			
3100-3110	BARREN																			
3110-3120	BARREN																			
3120-3130	BARREN																			
3130-3140	BARREN																			
3140-3150																				
3150-3160					P															
3160-3170																				
3170-3180															P					
3180-3190															P					
3190-3200				P	R				**P**				**P**		C					
3200-3210															P					
3210-3220	BARREN																			
3220-3230	BARREN																			
3230-3240	BARREN																			
3240-3250		P																		
3250-3260													P		P					
3260-3270																				P
3270-3280																				
3280-3290																				P
3290-3300	BARREN																			
3300-3310															R					
3310-3320																				
3320-3330															P					R
3330-3340																		P		
3340-3350													P		P					R
3350-3360			P												R					R
3360-3370					P	P									P					
3370-3380												P			R					P

Note: VA = Very Abundant, A = Abundant, C = Common, F = Few, R = Rare, P = Present. G = Good, M = Moderate, P = Poor. GM indicates a preservation status that falls between G and M and MP between M and P.

Appendix 1: Calcareous nannofossil distribution in Well L1, northern South China Sea.

Age	Zone	Interval	Sample depth (m)	Total abundance (100 FOVs)	Species richness	Number of *Discoaster* specimens	Preservation	*Blackites* sp.	*Calcidiscus leptoporus*	*Calcidiscus macintyrei*	*Calcidiscus premacintyrei*	*Calcidiscus tropicus*	*Clausicoccus subdistichus*	*Coccolithus miopelagicus*	*Coccolithus pelagicus*	*Coronocyclus nitescens*	*Cyclicargolithus abisectus*	*Cyclicargolithus floridanus*	*Discoaster challengeri*	*Discoaster deflandrei*	*Discoaster druggii*	*Discoaster exilis*	*Discoaster moorei*	*Discoaster petaliformis*	*Discoaster signus*	*Discoaster* sp. (5 rays)	*Discoaster* sp. (6 rays)	*Discoaster variabilis*	*Hayaster perplexus*	***Helicosphaera ampliaperta***	*Helicosphaera carteri*	*Helicosphaera euphratis*	*Helicosphaera obliqua*	*Helicosphaera recta*	*Helicosphaera* sp.	*Hughesius tasmaniae*	*Orthorhabdus serratus*	*Pontosphaera multipora*
Oligocene / Chattian	NP24 — ?	II	3380-3390	164	9	0	MP								F			F																				
			3390-3400	624	11	0	M								C			C																				
			3400-3410	423	15	0	M								F			C														P						R
			3410-3420	448	13	0	M						R		F			C																	P			
			3420-3430	243	13	0	M								F			F																	P	P		
			3430-3440	1	1	0	P											P																				
			3440-3450	3	4	0	MP											P																	P			
			3450-3460	2	2	0	MP								P			P																				
			3460-3470	21	9	0	MP								R			R																				
			3470-3480	0	0	0	BARREN																															
			3480-3490	2	2	0	M											P																				
			3490-3500	1	1	0	MP																															
			3500-3510	2	2	0	MP											P																				
			3510-3520	0	0	0	BARREN																															
			3520-3530	0	0	0																																
			3530-3540	1	1	0	P								P																							
			3540-3550	4	2	0	P								P			R																				
			3550-3560	2	2	0	MP											P																				
			3560-3570	3	2	0	MP											R																				
			3570-3580	2	2	0	P											P																				
			3580-3590	2	2	0	M											P																	P			
			3590-3600	0	0	0	BARREN																															
			3600-3610	0	0	0																																
			3610-3620	0	0	0																																
			3620-3630	0	0	0																																
			3630-3640	0	0	0																																
			3640-3650	0	0	0																																
			3650-3660	2	1	0	MP											P																				
			3660-3670	178	12	0	MP		P						F			F																	P			
			3670-3680	396	12	0	MP						P		F			C																				
			3680-3690	152	11	0	P						P		F			F																				
			3690-3700	125	9	0	MP						P		F			F																				
			3700-3710	9	7	0	MP											R																				
			3710-3720	0	0	0	BARREN																															
			3720-3730	0	0	0																																
			3730-3740	2	1	0	MP											R																				
			3740-3750	2	2	0	M											P																				
			3752-3755	0	0	0	BARREN																															
			3760-3770	0	0	0																																
			3770-3780	0	0	0																																
			3780-3790	1	1	0	M																															
			3790-3800	1	1	0	M																															
			3800-3810	0	0	0	BARREN																															
			3810-3820	0	0	0																																
			3820-3830	2	2	0	M											P																				
			3830-3840	93	7	0	MP								F			F																				
			3840-3850	10	4	0	M											R																				
			3850-3860	0	0	0	BARREN																															
			3860-3870	0	0	0																																
			3870-3880	0	0	0																																
			3880-3890	1	1	0	P											P																				
			3890-3900	0	0	0	BARREN																															
			3900-3910	164	11	1	M		P				P		F			F									P											
			3910-3920	1	1	0	MP											P																				
			3920-3930	13	5	0	M								P			P																				
			3930-3940	3	4	0	MP								P			P																				
			3940-3950	19	5	0	MP								P			F																				
			3950-3960	69	5	0	P								R			F																				
			3960-3970	902	18	1	MP								F		P	C									P							P	P			
			3970-3980	218	10	1	M						P		F			F									P											
?	Not zoned	I	3980-3990	4	4	0	MP								P			R																				
			3990-4000	0	0	0	BARREN																															
			4000-4010	0	0	0																																
			4010-4020	0	0	0																																

Sample depth (m)	*Pyrocyclus orangensis*	*Reticulofenestra ampla*	*Reticulofenestra bisecta*	***Reticulofenestra bisecta* (>10 μm)**	*Reticulofenestra bisecta filewiczii*	*Reticulofenestra haqii*	*Reticulofenestra lockeri*	*Reticulofenestra minuta*	*Reticulofenestra minutula*	*Reticulofenestra perplexa*	*Reticulofenestra pseudoumbilicus*	*Rhabdosphaera* sp.	***Sphenolithus belemnos***	*Sphenolithus calyculus*	*Sphenolithus capricornutus*	*Sphenolithus conicus*	***Sphenolithus delphix***	*Sphenolithus disbelemnos*	*Sphenolithus dissimilis*	***Sphenolithus distentus***	*Sphenolithus heteromorphus*	*Sphenolithus pospichalii*	*Sphenolithus moriformis*	***Sphenolithus predistentus***	*Sphenolithus procerus*	*Sphenolithus* sp.	***Triquetrorhabdulus carinatus***	*Triquetrorhabdulus milowii*	*Umbilicosphaera jafari*	*Umbilicosphaera rotula*	***Zygrhablithus bijugatus***
3380-3390		P						R	R														P	P		R					F
3390-3400		F					R	F	C	R	R									P				R		F					F
3400-3410		R	F			F	R	F	F							R				P			P	R		R					F
3410-3420							R	F	F		P									P			P	R		F					F
3420-3430		P				P	P	R	F		P													P		F					F
3430-3440																															
3440-3450							P																			P					
3450-3460																															
3460-3470						R		R	P				P			R					P					R					
3470-3480	BARREN																														
3480-3490										P																					
3490-3500																										P					
3500-3510																															P
3510-3520	BARREN																														
3520-3530																															
3530-3540																															
3540-3550																															
3550-3560									P																						
3560-3570										P																					
3570-3580											P																				
3580-3590																															
3590-3600	BARREN																														
3600-3610																															
3610-3620																															
3620-3630																															
3630-3640																															
3640-3650																															
3650-3660																															
3660-3670		R				R	R		R		R												R	P		F					
3670-3680		R				R	P	R	F		R					R				P				F		F					
3680-3690		R				P	R		R		R					P								R		F					
3690-3700		P						F	F		P													P		F					
3700-3710		R							R		P							P						P		R					
3710-3720	BARREN																														
3720-3730																															
3730-3740																															
3740-3750																										P					
3752-3755	BARREN																														
3760-3770																															
3770-3780																															
3780-3790									P																						
3790-3800		P																													
3800-3810	BARREN																														
3810-3820																															
3820-3830									P																						
3830-3840		P					P	F	F																	P					
3840-3850						P										P										P					
3850-3860	BARREN																														
3860-3870																															
3870-3880																															
3880-3890																															
3890-3900	BARREN																														
3900-3910							P	F	F		P													P		F					
3910-3920																															
3920-3930								P	P															P							
3930-3940											P															P					
3940-3950		P							R																	P					
3950-3960		P							R																	F					
3960-3970		F		P		F	P	F	C	R	F					F				P				R		C					P
3970-3980		F				P			F		F															F					P
3980-3990									P		P																				
3990-4000	BARREN																														
4000-4010																															
4010-4020																															

Note: VA = Very Abundant, A = Abundant, C = Common, F = Few, R = Rare, P = Present. G = Good, M = Moderate, P = Poor. GM indicates a preservation status that falls between G and M and MP between M and P.

Appendix 1: Calcareous nannofossil distribution in Well L1, northern South China Sea (continued).

Age	Zone	Interval	Sample depth (m)	Total abundance (100 FOVs)	Species richness	Number of *Discoaster* specimens	Preservation	*Blackites* sp.	*Calcidiscus leptoporus*	*Calcidiscus macintyrei*	*Calcidiscus premacintyrei*	*Calcidiscus tropicus*	*Clausicoccus subdistichus*	*Coccolithus miopelagicus*	*Coccolithus pelagicus*	*Coronocyclus nitescens*	*Cyclicargolithus abisectus*	*Cyclicargolithus floridanus*
Oligocene (?) Undetermined	Not zoned	I	4020-4030	2	2	0	MP											P
			4030-4040	4	4	0	MP								P			P
			4040-4050	5	4	0	MP								R			R
			4050-4060	0	0	0	BARREN											
			4060-4070	8	4	0	MP								R			F
			4070-4080	14	6	0	MP								R			R
			4080-4090	14	5	0	MP								F			F
			4090-4100	17	8	0	MP						P		F			F
			4100-4110	12	6	0	M								P			R
			4110-4120	7	5	0	P								P			P
			4120-4130	4	4	0	MP								P			P
			4130-4140	2	2	0	P											P
			4140-4150	5	3	0	M								R			R
			4150-4160	3	3	2	P											
			4160-4170	6	5	0	MP								P			R
			4170-4180	8	6	0	M						P		P			P
			4180-4190	6	4	0	MP								P			R
			4190-4200	6	4	0	P								P			R
			4200-4210	8	5	0	P								P			R
			4210-4220	3	3	0	P											P
			4220-4230	2	1	0	P											
			4230-4240	1	1	0	MP											P
			4240-4250	6	6	0	MP											R
			4250-4260	4	4	0	MP								P			P
			4260-4270	5	4	0	MP								P			R
			4270-4280	3	3	1	MP		P									
			4280-4290	4	4	1	MP								P			P
			4290-4300	4	4	0	MP								P			P
			4300-4310	7	5	1	MP								P			P
			4310-4320	6	4	1	MP								P			P
			4320-4330	4	3	0	MP											P
			4330-4340	4	4	1	M								P			P
			4340-4350	4	3	0	M											R
			4350-4360	2	2	0	MP											P
			4360-4370	8	6	0	M								P			R
			4370-4380	6	5	0	M								P			R
			4380-4390	3	2	0	MP											P
			4390-4400	4	4	0	M								P			P
			4400-4410	2	2	0	P											P
			4410-4420	1	1	0	P											
			4420-4430	2	1	0	P											P
			4430-4440	4	3	0	MP											R
			4440-4450	11	9	1	M								P			R
			4450-4460	1	1	0	P											P
			4460-4470	0	0	0	BARREN											
			4470-4480	0	0	0	BARREN											
			4480-4485	1	1	0	P								P			
			4490-4500	0	0	0	BARREN											
			4500-4505	1	1	0	M											P
			4510-4520	1	1	0	M											P
			4520-4530	0	0	0	BARREN											
			4530-4540	1	1	0	M											
			4540-4550	1	1	0	MP											P
			4550-4558	0	0	0	BARREN											
			4560-4563	0	0	0	BARREN											
			4570-4580	0	0	0	BARREN											
			4580-4590	0	0	0	BARREN											
			4590-4600	2	1	0	M											P
			4600-4603	2	2	0	P								P			P
			4610-4620	0	0	0	BARREN											
			4620-4630	1	1	0	P								P			
			4630-4640	1	1	0	P											P
			4640-4650	2	1	0	M											

Sample depth (m)	*Discoaster challengeri*	*Discoaster deflandrei*	*Discoaster druggii*	*Discoaster exilis*	*Discoaster moorei*	*Discoaster petaliformis*	*Discoaster signus*	*Discoaster* sp. (5 rays)	*Discoaster* sp. (6 rays)	*Discoaster variabilis*	*Hayaster perplexus*	***Helicosphaera ampliaperta***	*Helicosphaera carteri*	*Helicosphaera euphratis*	*Helicosphaera obliqua*	*Helicosphaera recta*	*Helicosphaera* sp.	*Hughesius tasmaniae*	*Orthorhabdus serratus*	*Pontosphaera multipora*	*Pyrocyclus orangensis*
4020-4030																					
4030-4040																					
4040-4050																					
4050-4060	BARREN																				
4060-4070																					
4070-4080																					
4080-4090																					
4090-4100																					
4100-4110																					
4110-4120																					
4120-4130																					
4130-4140																					
4140-4150																					
4150-4160		P						P													
4160-4170																	P				
4170-4180																					
4180-4190																					
4190-4200																					
4200-4210																					
4210-4220																					
4220-4230																					
4230-4240																					
4240-4250																					
4250-4260																					
4260-4270																					
4270-4280									P												
4280-4290									P												
4290-4300																					
4300-4310									P												
4310-4320									P												
4320-4330																					
4330-4340									P												
4340-4350																					
4350-4360																					
4360-4370																					
4370-4380																					
4380-4390																					
4390-4400																					
4400-4410																					
4410-4420																					
4420-4430																					
4430-4440																					
4440-4450									P				P								
4450-4460																					
4460-4470	BARREN																				
4470-4480	BARREN																				
4480-4485																					
4490-4500	BARREN																				
4500-4505																					
4510-4520																					
4520-4530	BARREN																				
4530-4540																					
4540-4550																					
4550-4558	BARREN																				
4560-4563	BARREN																				
4570-4580	BARREN																				
4580-4590	BARREN																				
4590-4600																					
4600-4603																					
4610-4620	BARREN																				
4620-4630																					
4630-4640																					
4640-4650																					

Sample depth (m)	*Reticulofenestra ampla*	*Reticulofenestra bisecta*	***Reticulofenestra bisecta* (>10 µm)**	*Reticulofenestra bisecta filewiczii*	*Reticulofenestra hagii*	*Reticulofenestra lockeri*	*Reticulofenestra minuta*	*Reticulofenestra minutula*	*Reticulofenestra perplexa*	*Reticulofenestra pseudoumbilicus*	*Rhabdosphaera* sp.
4020-4030	P										
4030-4040								P			
4040-4050								P			
4050-4060	BARREN										
4060-4070								P		P	
4070-4080	R				P			F		R	
4080-4090								F		R	
4090-4100	R					P		F		R	
4100-4110							P	R		P	
4110-4120								R		P	
4120-4130								P			
4130-4140								P			
4140-4150											
4150-4160											
4160-4170								P			
4170-4180					P			P			
4180-4190	P							R			
4190-4200								P			
4200-4210								P		P	
4210-4220										P	
4220-4230											
4230-4240											
4240-4250					P			P		P	
4250-4260							P	P			
4260-4270								P			
4270-4280								P			
4280-4290								P			
4290-4300							P	P			
4300-4310								P			
4310-4320								P			
4320-4330								P			
4330-4340								P			
4340-4350								P		R	
4350-4360								P			
4360-4370							P	P	P		
4370-4380					P			R		P	
4380-4390								P			
4390-4400								P			
4400-4410								P			
4410-4420								P			
4420-4430											
4430-4440								P			
4440-4450	P			P				R			
4450-4460											
4460-4470	BARREN										
4470-4480	BARREN										
4480-4485											
4490-4500	BARREN										
4500-4505											
4510-4520											
4520-4530	BARREN										
4530-4540								P			
4540-4550											
4550-4558	BARREN										
4560-4563	BARREN										
4570-4580	BARREN										
4580-4590	BARREN										
4590-4600											
4600-4603											
4610-4620	BARREN										
4620-4630											
4630-4640											
4640-4650								P			

Sample depth (m)	***Sphenolithus belemnos***	*Sphenolithus calyculus*	*Sphenolithus capricornutus*	*Sphenolithus conicus*	***Sphenolithus delphix***	*Sphenolithus disbelemnos*	*Sphenolithus dissimilis*	***Sphenolithus distentus***	*Sphenolithus heteromorphus*	*Sphenolithus moriformis*	*Sphenolithus pospichalii*	***Sphenolithus predistentus***	*Sphenolithus procerus*	*Sphenolithus* sp.	***Triquetrorhabdulus carinatus***	*Triquetrorhabdulus milowii*	*Umbilicosphaera jafari*	*Umbilicosphaera rotula*	***Zygrhablithus bijugatus***
4020-4030																			
4030-4040														P					
4040-4050														P					
4050-4060	BARREN																		
4060-4070																			
4070-4080																			
4080-4090														P					
4090-4100														R					
4100-4110														R					
4110-4120														R					
4120-4130														P					
4130-4140																			
4140-4150														P					
4150-4160														P					
4160-4170														P					
4170-4180														P					
4180-4190																			
4190-4200														P					
4200-4210														P					
4210-4220														P					
4220-4230														P					
4230-4240																			
4240-4250				P										P					
4250-4260																			
4260-4270														P					
4270-4280																			
4280-4290																			
4290-4300																			
4300-4310														P					
4310-4320																			
4320-4330														P					
4330-4340																			
4340-4350																			
4350-4360																			
4360-4370														P					
4370-4380																			
4380-4390																			
4390-4400														P					
4400-4410																			
4410-4420																			
4420-4430																			
4430-4440														P					
4440-4450										P				R					
4450-4460																			
4460-4470	BARREN																		
4470-4480	BARREN																		
4480-4485																			
4490-4500	BARREN																		
4500-4505																			
4510-4520																			
4520-4530	BARREN																		
4530-4540																			
4540-4550																			
4550-4558	BARREN																		
4560-4563	BARREN																		
4570-4580	BARREN																		
4580-4590	BARREN																		
4590-4600																			
4600-4603																			
4610-4620	BARREN																		
4620-4630																			
4630-4640																			
4640-4650																			

Note: VA = Very Abundant, A = Abundant, C = Common, F = Few, R = Rare, P = Present. G = Good, M = Moderate, P = Poor. GM indicates a preservation status that falls between G and M and MP between M and P.

Appendix 1: Calcareous nannofossil distribution in Well L1, northern South China Sea (continued).